ORIGINAL PAPER

Chengguo Hu · Shengshui Hu

Electrochemical characterization of cationic surfactants' adsorption on a disturbed n-alkanethiolate self-assembled monolayer-modified polycrystalline gold electrode

Abstract The adsorption of cetyltrimethylammonium bromide (CTAB) on disturbed n-alkanethiolate self-assembled monolayers (SAMs) was investigated by electrochemical methods with potassium ferricyanide [$K_3Fe(CN)_6$] as a probe. Compared with the completely restrained signal at ordinary compact n-alkanethiolate SAMs, the electrochemical response of $K_3Fe(CN)_6$ at the disturbed n-alkanethiolate SAMs was partly restored and became progressively reversible in the presence of increasing concentrations of CTAB, which was employed to characterize the adsorption of cationic surfactants on hydrophobic SAMs. The effect of CTAB concentration on electrochemical impedance spectroscopy (EIS) plots indicated that CTAB experienced two different types of adsorptive behavior at the disturbed n-alkanethiolate SAMs: monomer adsorption at low concentrations below 1×10^{-6} M and monolayer adsorption at CTAB concentrations above 1×10^{-5} M. The adsorption of a series of cationic surfactants with similar structures to CTAB on disturbed n-alkanethiolate SAMs was also explored. These surfactants had similar adsorptive behavior and showed nearly linear adsorption characteristics with the length of their hydrophobic tails.

Keywords n-Alkanethiolates · Cationic surfactant · Electrochemical methods · Hydrophobic adsorption · Self-assembled monolayers
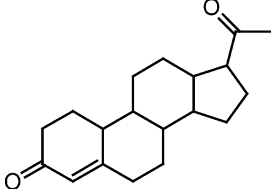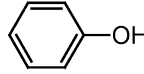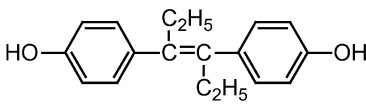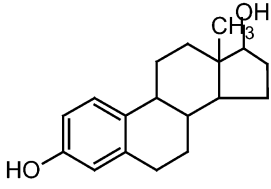
Introduction

Surfactants are a kind of amphiphilic molecule with a polar head on one side and a long hydrophobic tail on

C. Hu · S. Hu (✉)
Department of Chemistry, Wuhan University, 430072 Wuhan, PR China
E-mail: sshu@whu.edu.cn
Tel.: +86-27-87218904
Fax: +86-27-87647617

the other. The special properties of their structures determine that these molecules spontaneously adsorb on interfaces made up of two phases with different polarities or concentrate into micelles in solution. The applications of surfactants in electrochemistry and electroanalytical chemistry have been widely reported [1]. Hu's group [2, 3, 4, 5] has used surfactants in electroanalytical chemistry to improve the detection limits of some biomolecules. The experimental results showed that the electrochemical responses of these compounds were greatly enhanced (see Table 1). It can be seen that the presence of trace surfactants improved the sensitivities of these biomolecules by at least five times. A "synergistic adsorption" mechanism was proposed to interpret these enhancement effects of surfactants, i.e. surfactants might combine with the substrates in certain forms and strengthen their adsorption on the electrode surface, which facilitates the electron or substance transfer between the electrode and the solution. Besides the addition of surfactants to the working solutions, some researchers blended surfactants into the electrode matrixes or dispersed surfactants on the electrode surface to prepare chemically modified electrodes. Digua et al. [6, 7] and Posac et al. [8] mixed the amphiphile hexadecylsulfonic acid into carbon paste to produce a chemically modified carbon paste electrode. This electrode exhibited a strong cation exchange property and showed an improved electron transfer rate between the substrates and the electrode. Falaras et al. [9], Nassar et al. [10] and Carrero and León [11] prepared an organoclay-modified glassy carbon electrode coated with a cationic surfactant bilayer. They found that this electrode possessed anion-exchange ability and could accumulate both negatively charged metal complexes and neutral redox active reagents. We have developed a cetyltrimethylammonium bromide (CTAB) modified carbon paste electrode based on surface modification methods [12]. The electrochemical response of $K_3Fe(CN)_6$ at this electrode revealed that CTAB formed a stable monolayer on the electrode surface, based on the hydrophobic interaction between the hydrophobic

Table 1 Enhancement effects of surfactants on the electrochemical responses of some biomolecules

Compounds	Structure	Concentration (M)	Electrode	Surfactant	$I_a(\mu A)$[a]	$I_p(\mu A)$[b]
Progesterone[2]		1×10^{-6}	DME	1×10^{-4}M CTAB	0	1.5
Phenol[3]		2×10^{-6}	Nafion/GCE	6×10^{-5}M CTAB	10	60
Diethylstilbestrol[4]		4×10^{-5}	CPE	1.2×10^{-4}M CPB	2.5	25
Estrodiol[5]		4×10^{-5}	Nafion/GCE	6×10^{-5}M CTAB	20	250

[a]The peak current of biomolecules in the absence of surfactants
[b]The peak current of biomolecules in the presence of surfactants

long chain of CTAB and the paraffin oil in the carbon paste. The appearance of large redox peak currents at low concentrations of $K_3Fe(CN)_6$ also indicated that many defects existed in the CTAB film on a carbon paste electrode, due to the complex surface property of such electrodes.

Some less soluble surfactants have been employed in the immobilization of macromolecules or other functional materials. Wu et al. [13] developed stable multi-wall carbon nanotube (MWNT) modified electrodes based on the immobilization of MWNTs in a film of insoluble dihexadecyl phosphate (DHP) on a glassy carbon electrode. This electrode showed electrocatalytical activity toward trace substances and has been used as a sensor for the determination of biomolecules [14, 15]. The applications of surfactants in the immobilization of biomolecules have also been reported [16, 17, 18]. Chattopadhyay et al. [19] studied the direct electrochemistry of heme proteins at a neutral surfactant modified glassy carbon electrode. The results showed that surfactant molecules interacted with the electrode surface in a specific manner and anchored the protein molecules to align in a suitable orientation, which promoted electron transfer between the protein molecules and the glassy carbon electrode.

Contrary to the extensive applications of surfactants in electroanalytical chemistry and electrochemistry, little research has been carried out to explore the nature of surfactant adsorption on electrode surfaces. Hu et al.

[20] have characterized the adsorption of sodium dodecyl sulfate (SDS) on both charge-regulated and hydrophobic substrates by atomic force microscopy force measurement. They found that the interaction between SDS and the positively charged electrode surface was a strong function of SDS concentration. Moreover, with the increase of concentration, SDS showed different adsorptive behavior on the hydrophobic electrode surface, including monomer adsorption and monolayer adsorption. These results were consistent with the conclusions drawn by Montgometry and Wirth [21] using spectroscopic methods. Sigal et al. [22] used surface plasmon resonance spectroscopy to measure the association of surfactants with hexadecanethiolate self-assembled monolayers (SAMs) on gold. The adsorption of surfactants with hydrophobic SAMs was described well by the Langmuir adsorption isotherm. Although these techniques were powerful tools for characterizing the adsorption of various surfactants on solid surfaces, the apparatuses employed were expensive and the operations were complicated. Moreover, these systems were unfit for electrochemical research because the hydrophobic layers on the solid backstop were regulated and compact, which completely blocked approaches of the electrochemical probes to the electrode surfaces.

To our knowledge, no research involved in the electrochemical characterization of the adsorption of surfactants on ordinary n-alkanethiolate SAMs has been reported because of the completely restrained responses

of electrochemical probes at these electrodes. In this paper, we propose an electrochemical method for the characterization of cationic surfactants' adsorption on disturbed n-alkanethiolate SAMs, which allowed electrochemical probes to pass through the hydrophobic film of the n-alkanethiolate via the defects produced during sonication in water. Compared with ordinary dense and regulated n-alkanethiolate SAMs, the SAMs sonicated in water might have many more defects, reflected by the reappearance of the $K_3Fe(CN)_6$ response. In the presence of cationic surfactants, both the reversibility and the sensitivity of $K_3Fe(CN)_6$ were apparently improved. This phenomenon was used to characterize the adsorption of surfactants on the hydrophobic electrode surface. The results may help us to understand the role of surfactants in electrochemistry and their adsorptive behavior on hydrophobic solid surfaces.

Experimental

Chemicals

Lauryltrimethylammonium bromide (LTAB), cetylpyridinium bromide (CPB), cetyltrimethylammonium bromide (CTAB) and stearyltrimethylammonium bromide (STAB) (purchased from Shanghai Reagent, China) were dissolved in water to prepare 1×10^{-2} M stock solutions. Dodecanethiol ($>98.0\%$) from Shanghai Reagent was dissolved in absolution ethanol to form a 4 mM solution for the self-assembly process. Potassium ferricyanide [$K_3Fe(CN)_6$] was obtained from Beijing Reagent and was dissolved in water to form a 0.1 M stock solution. All chemicals were of analytical grade quality except for dodecanethiol and were used without further purification. The water used was double-distilled water.

Apparatus and procedure

Cyclic voltammograms and chronocoulometry were performed using an EG&G model 283 electrochemical workstation (Princeton Applied Research, USA) controlled by M270 software and linked to a P4 computer. Electrochemical impedance spectroscopy (EIS) was carried out with the EG&G model 283 electrochemical workstation and an EG&G model 5210 lock-in amplifier (Princeton Applied Research) powered by Powersuit software. The equivalent circuit was deduced using ZsimpWin software produced by Echem Software. All the experiments were carried out in a conventional electrochemical cell. The electrode system contained a disturbed n-alkanethiolate SAM-modified polycrystalline gold disk working electrode (CHI, 2 mm in diameter), a platinum wire counter electrode and a potassium chloride (KCl) saturated calomel reference electrode (SCE). In EIS, the frequency range was from 100 mHz to 100 kHz, the DC potential was 0.12 V vs. SCE and

the amplitude was 10 mV. The parameters in chronocoulometry were as follows: initial potential 0.35 V, final potential −0.05 V, pulse width 4 s. Prior to the measurements, the working electrode was kept quiet for 6–10 min to ensure equilibrium. The electrolyte used in all measurements was an aqueous solution of 0.05 M KCl containing 20% acetone (v/v).

Preparation of n-alkanethiolate SAM-modified polycrystalline gold electrode

The gold electrode was firstly polished on a slush of 0.05 μm alumina (Al_2O_3). Then this electrode was sonicated in water for 5 min and scanned in 1 M H_2SO_4 in the potential range of −0.2 to 1.5 V until stable signals were obtained. The area of the reduction peak at each bare gold electrode was compared to ensure that all the SAM-modified gold electrodes had the same effective area. Then the gold electrode was sonicated for 5 min in water and ethanol, successively.

The above electrode was immersed in 4 mM ethanol solution of dodecanethiol and kept overnight. For an ordinary SAM-modified gold electrode, the electrode was taken out from the dodecanethiol solution and sonicated in ethanol for 10 min to remove any physical adsorbate. As for the disturbed SAM-modified electrode, the ordinary SAM-modified electrode was further sonicated in water for another 10 min and dried with nitrogen gas. The sonication of ordinary SAMs in water may produce many defects in the compact SAM film because the orientation of long hydrophobic chains of alkanethiolate SAMs on a solid in the presence of water is different from that in the presence of organic solvents [21, 23, 24].

Results and discussion

Voltammetric responses of $K_3Fe(CN)_6$ at a disturbed dodecanethiolate SAM-modified polycrystalline gold electrode in the presence of CTAB

Figure 1 shows the cyclic voltammograms of $K_3Fe(CN)_6$ at a disturbed n-alkanethiolate SAM-modified gold electrode in the presence of CTAB. Compared with the well-defined redox peaks at a bare gold electrode (curve a), the electrochemical response of $K_3Fe(CN)_6$ at an ordinary alkanethiolate SAM-modified gold electrode (curve e) is completely repressed, due to the block of mass transfer by the regulated compact hydrophobic layer of the SAM. In the presence of CTAB, no apparent response of $K_3Fe(CN)_6$ is observed (curve c). However, when the above SAM-modified gold electrode is sonicated in water for 10 min (the resulting electrode is referred to as the disturbed SAM-modified electrode), the response of $K_3Fe(CN)_6$ is partly restored (curve d). In the presence of CTAB, the signal for $K_3Fe(CN)_6$ is apparently improved (curve b). The reappearance of the electrochemical response of $K_3Fe(CN)_6$ at the disturbed
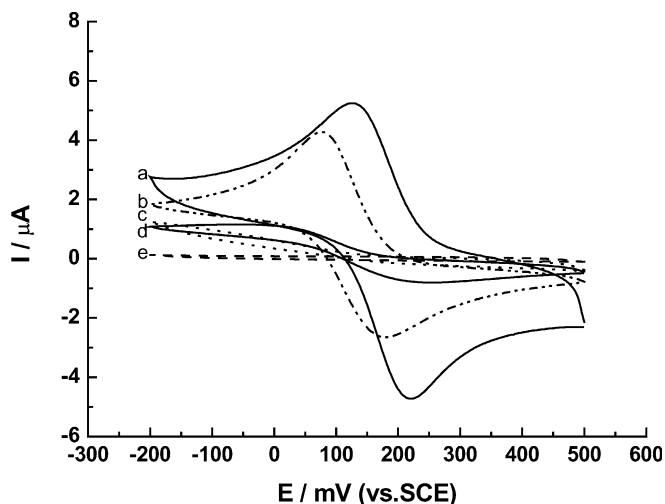
Fig. 1 Cyclic voltammograms of 1 mM $K_3Fe(CN)_6$ at: (*a*) a bare gold electrode; (*b*) a disturbed n-dodecanethiolate SAM-modified gold electrode in the presence of 1×10^{-5} M CTAB; (*c*) an ordinary n-dodecanethiolate SAM-modified gold electrode in the presence of 1×10^{-5} M CTAB; (*d*) a disturbed n-dodecanethiolate SAM-modified gold electrode; (*e*) an ordinary n-dodecanethiolate SAM

Fig. 2 Effect of CTAB concentration on the voltammetric response of 1 mM $K_3Fe(CN)_6$ at a disturbed n-dodecanethiolate SAM-modified gold electrode. The CTAB concentration from curves (*a*) to (*g*) was 0, 1, 3, 5, 10, 45 and 100 μM, respectively

SAM-modified gold electrode might arise from the appearance of defects in the SAM film produced during sonication in water, which allows the electrochemical probe to pass through the thick insulated film and reach the electrode surface. The linear relationships of both the reduction and the oxidation peak currents with scan rate showed that either $K_3Fe(CN)_6$ or $K_4Fe(CN)_6$ underwent an adsorption-controlled process at a disturbed SAM-modified gold electrode in the presence of CTAB. By comparing the behavior of $K_3Fe(CN)_6$ in the presence and absence of CTAB, it is obvious that $K_3Fe(CN)_6$ is indirectly adsorbed on to the electrode surface with the aid of CTAB, i.e. the voltammetric response of $K_3Fe(CN)_6$ in the presence of CTAB can be utilized to characterize the adsorptive behavior of CTAB on a disturbed n-alkanethiolate SAM-modified gold electrode.

Figure 2 shows the effect of CTAB concentration on the cyclic voltammetric responses of $K_3Fe(CN)_6$ at a disturbed SAM-modified gold electrode. With the increase of CTAB concentration, the response of the $K_3Fe(CN)_6$ is gradually improved. The effects of CTAB concentration on the redox peak currents and the peak potentials (E_p) are shown in Fig. 3. When the CTAB concentration is lower than 1×10^{-6} M, both the redox peak potentials (Fig. 3a) and the peak currents (Fig. 3b) alter little. According to Hu et al.'s report [20], CTAB may undergo monomer adsorption in this concentration range. In the range of 1×10^{-6} M to 1×10^{-5} M, the difference of the peak potentials and the peak currents changes rapidly, which suggests variation of the CTAB adsorptive behavior. With a further increase of CTAB concentration, the redox peak potential and the oxidation peak current tend to be stable. The different behavior of the reduction and oxidation peak currents
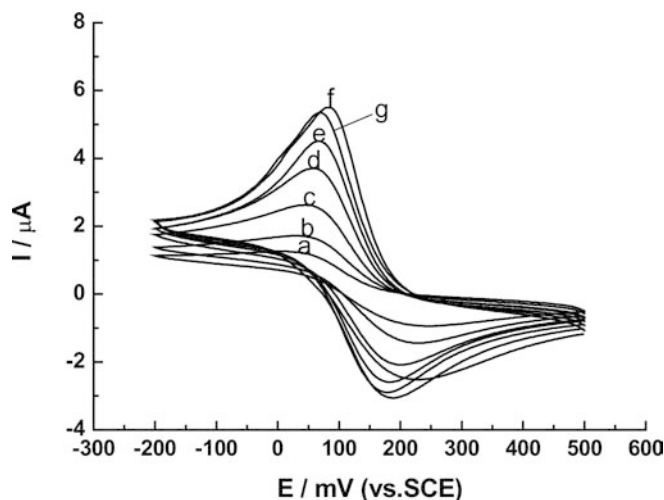
can be interpreted by the change of the electronic configuration and the geometry of the ion pairs formed by $K_3Fe(CN)_6$ and CTAB during the reduction process [25]. At this concentration, CTAB might form a loose monolayer on the SAM. When the CTAB concentration is higher than 6.5×10^{-5} M, the response of $K_3Fe(CN)_6$ declines. Under this condition, the ion pairs of CTAB and $K_3Fe(CN)_6$ may be precipitated from solution to the electrode surface and block the mass transfer of $K_3Fe(CN)_6$. In fact, when the CTAB concentration was too high, obvious deposits could be observed in the solution. Over the whole concentration range, the adsorption of CTAB on disturbed SAMs was weak and the rate of adsorption/desorption was fast.

Chronocoulometry of CTAB adsorption
on a disturbed n-alkanethiolate SAM-modified
gold electrode

The adsorption of CTAB on hydrophobic SAMs was achieved through the hydrophobic interaction between the long chains of CTAB and the alkanethiolate, i.e. interchain penetration. With the increase of CTAB concentration, the adsorption ability of CTAB on SAMs was enhanced and the penetration between CTAB and the alkanethiolate increased, which resulted in the condensation of the hydrophobic layer [21]. If electrochemical probes were present in the solution, the presence of surfactants in the solution may inhibit the diffusion of the probes. It is well known that chronocoulometry can be used to measure the apparent diffusion coefficient (D_{app}). Thus, chronocoulometry was employed to further estimate the adsorption of CTAB on a disturbed n-alkanethiolate SAM-modified gold electrode.

Figure 4 shows the effect of CTAB concentration on the chronocoulometry of $K_3Fe(CN)_6$. With the increase
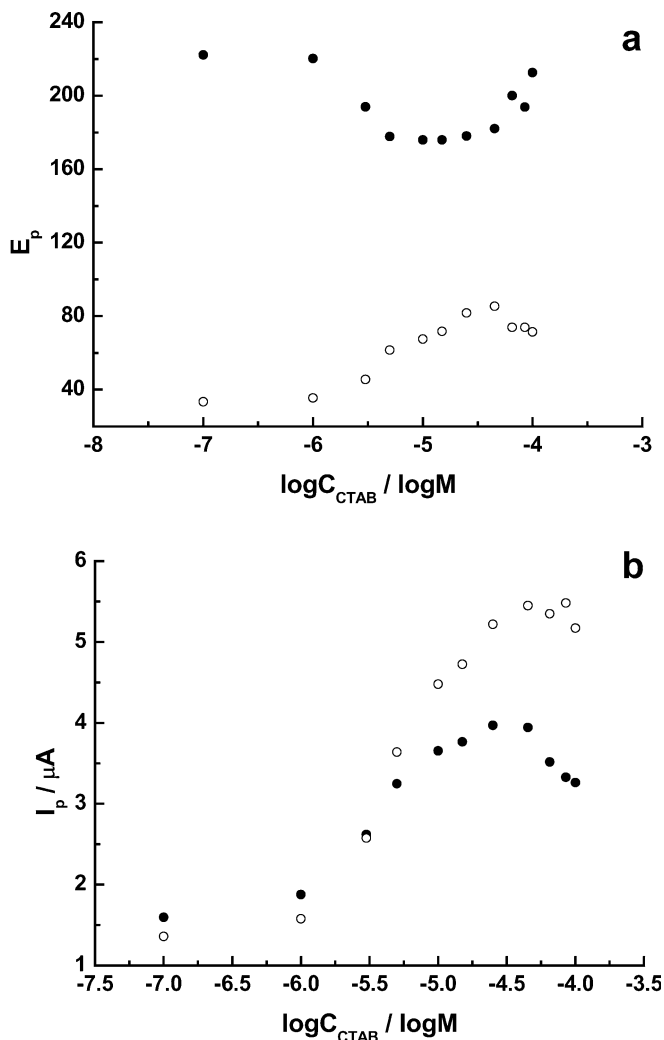
Fig. 3 Variation of the redox peak potentials (a) and peak currents (b) of 1 mM $K_3Fe(CN)_6$ at a disturbed n-dodecanethiolate SAM-modified gold electrode with CTAB concentration for the reduction (*open circles*) and the oxidation (*filled circles*) processes

Fig. 4 Chronocoulometry of 1 mM $K_3Fe(CN)_6$ at a disturbed n-dodecanethiolate SAM-modified gold electrode in the presence of (from *a* to *h*): 0.1, 1, 3, 5, 10, 25, 45 and 100 μM CTAB, respectively. The *inset* shows the linear relationship between D_{app} and CTAB concentration

trode in the determination of surfactant concentrations has been reported previously [25, 26, 27].

Electrochemical impedance characterization of CTAB adsorption on a disturbed n-alkanethiolate SAM-modified gold electrode

To investigate the structure of the electrode interface, EIS was performed. A typical EIS plot for a semi-infinite system contains a semicircle in the high-frequency region and a declining line with a slope of 1 in the low-frequency region. The semicircle in the EIS plot corresponds to a dynamic process, while the declining line stands for a diffusion process. From the composition of the EIS plot, useful information involved in the interface structure and important parameters about the dynamic process can be conveniently deduced.

Figure 5 shows the EIS plot of $K_3Fe(CN)_6$ at a disturbed SAM in the presence of 1×10^{-5} M CTAB. The Nyquist plot (Fig. 5a) comprises an incomplete semicircle at high frequencies and a declining line at low frequencies, which suggests that the electrochemical reaction of $K_3Fe(CN)_6$ under this condition is controlled by both the dynamic and the diffusion processes. As for the Bode plot (Fig. 5b), only one peak is observed, indicating that only one semicircle exists in the semicircle of the Nyquist plot. Thus, the intercept of the incomplete semicircle on the horizon axis could be used to estimate the charge transfer resistance (R_{ct}) of $K_3Fe(CN)_6$ at the disturbed SAMs in the presence of CTAB.

It is clear that both the Nyquist plot and the Bode plot could be well fitted by a modified Randle's circuit. This equivalent circuit is schematically represented in Fig. 6. The equivalent circuit consists of two resistances and two constant phase angle elements (CPEs).

of CTAB concentration, the chronocoulometry of $K_3Fe(CN)_6$ varies regularly. In the range of 1×10^{-7} M to 1×10^{-4} M, the charge (Q) exhibits a good linear relationship with the square root of time ($t^{1/2}$). According to the integrated Cottrell equation:

$$Q = \frac{2nFAC^bD^{1/2}t^{1/2}}{\pi^{1/2}}$$ (1)

where $n=1$, $A=0.0314$ cm^2 and $C^b=1$ mol/cm^3; thus the D_{app} of $K_3Fe(CN)_6$ in the presence of various concentrations of CTAB can be obtained. It is interesting that D_{app} decreases linearly with the increase of CTAB concentration (inset of Fig. 4), indicating the increase of the density of the hydrophobic film or the decrease of free $K_3Fe(CN)_6$ in solution by forming ion pairs with CTAB. The above linear relationship can be used to estimate the concentration of the surfactants. The application of a n-alkanethiolate SAM-modified elec-
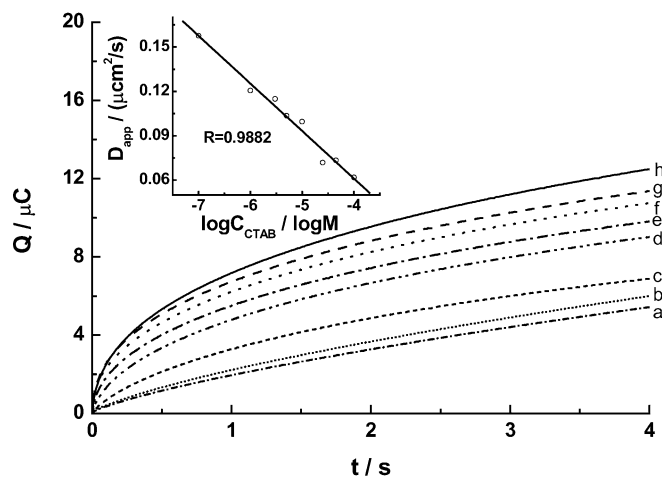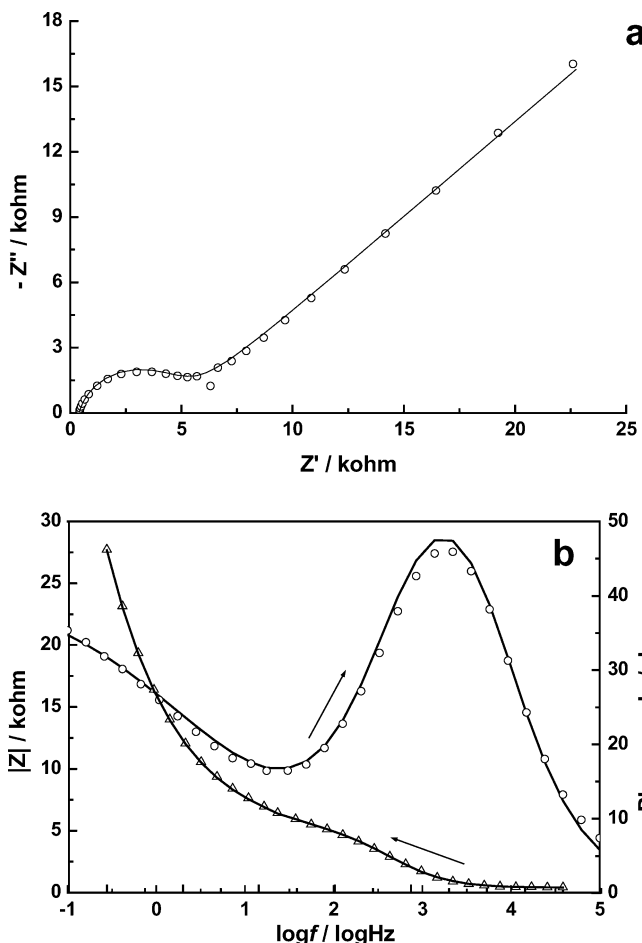
Fig. 5 The EIS plots of 1 mM $K_3Fe(CN)_6$ at a disturbed n-dodecanethiolate SAM-modified gold electrode in the presence of 1×10^{-5} M CTAB: (**a**) Nyquist plot; (**b**) Bode plot. The *solid lines* in the plots are the fitting lines obtained from an equivalent circuit

Generally, the impedance of a CPE (Z_{CPE}) can be described by the following equation:

$$Z_{CPE} = \frac{1}{Y_0}(j\omega)^{-\phi} \qquad (2)$$

where Y_0 (the admittance parameter, S cm^{-2} s$^{-\phi}$) and ϕ (a dimensionless exponent) are two parameters independent of the frequency, and ω (Hz) is the angle frequency. The admittance parameter Y_0 is not a constant but represents a product depending on the type of CPE. When $n=0$, the CPE is reduced to a resistance; when
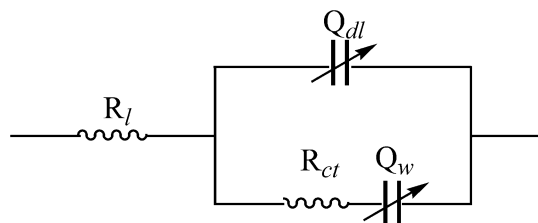

Fig. 6 The schematic representation of the equivalent circuit mentioned in Fig. 5

$n=1$, the CPE could be regarded as a capacitor, for which the impedance can be expressed as [28]:

$$Z_{CPE}^{C} = (j\omega)^{\phi_{dl}-1} C_{dl}^{\phi_{dl}-1} R_l^{\phi_{dl}} \qquad (3)$$

When $n=0.5$, the CPE is equal to a mass transfer impedance (Warburg impedance), which is in relation to the diffusion process. According to Retter et al. [29], the CPE for Warburg impedance is:

$$Z_{CPE}^{W} = R_{ct}^{1-2\phi_w} 2^{\phi_w} \sigma^{2\phi_w}(j\omega)^{-\phi_w} \qquad (4)$$

In Eqs. 3 and 4, C_{dl} is the capacitor of the electric double layer and σ is the Warburg coefficient. The use of the CPE to replace the capacitor is to compensate for the deviation of the actual electrode interface from a pure capacitor. For the two resistances, R_l refers to the solution resistance and R_{ct} is the charge transfer resistance of the electrochemical reaction. As for the two CPEs, Q_{dl} is used to describe the capacitor of the electric double layer of the electrode interface and Q_w
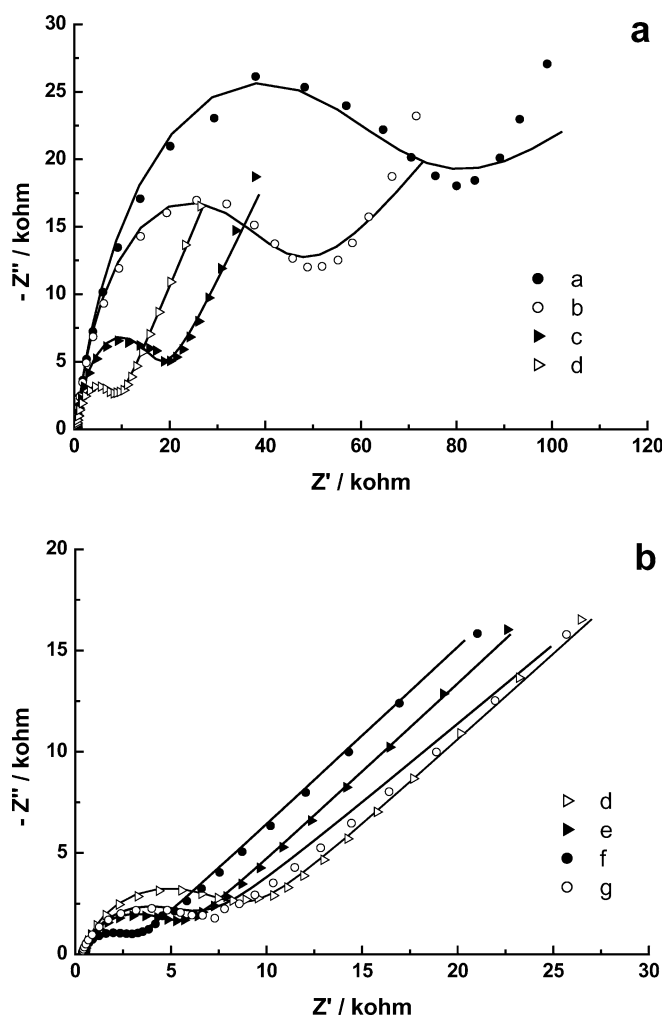

Fig. 7 Effect of CTAB concentration on the Nyquist plot of 1 mM $K_3Fe(CN)_6$ at a disturbed n-dodecanethiolate SAM-modified gold electrode. CTAB concentrations from curve *a* to curve *g* were 0, 0.1, 3, 5, 10, 25 and 65 μM, respectively
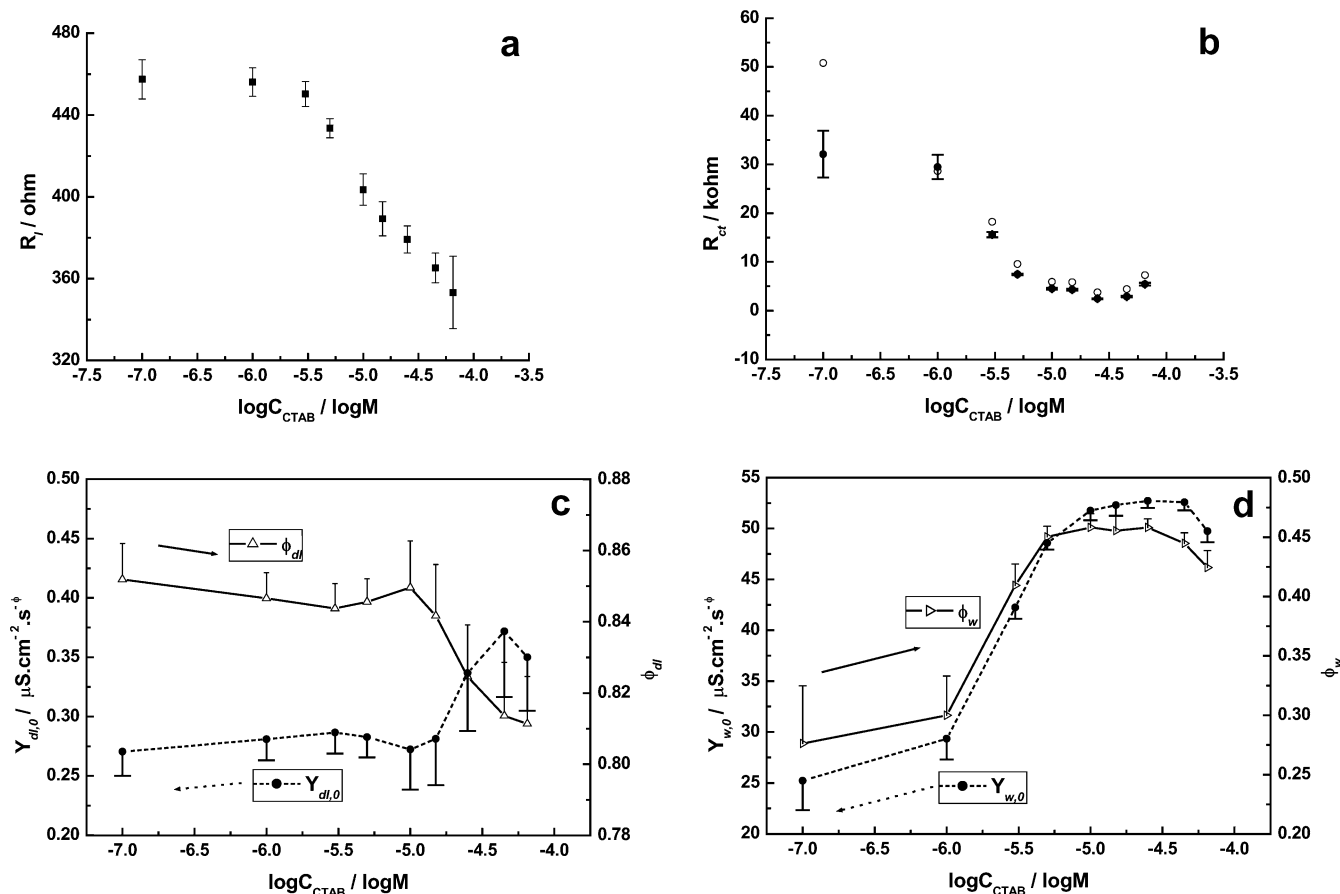
Fig. 8 Effect of CTAB concentration on the equivalent elements in Fig. 6: (a) R_l; (b) R_{ct}; (c) Q_{dl}; (d) Q_w. The data in (b) were measured from the intercepts of the semicircles on Nyqusit plots (*filled circles*) and from the equivalent circuit (*open circles*)

is used to express the impedance involved in the diffusion process.

The effect of CTAB concentration on the voltammetric responses of $K_3Fe(CN)_6$ at disturbed SAMs indicate that CTAB could apparently affect the property of the electrode surface. However, the information on the structure of the electrode surface obtained from voltammetric plots is limited. Here, EIS is employed to characterize the effect of CTAB concentration on the structure of the electrode surface. Figure 7 shows the effect of CTAB concentration on EIS plots for $K_3Fe(CN)_6$. Apparently, the diameters of the semicircles on the Nyquist plot decrease with the increase of CTAB concentration at first. When the CTAB concentration reaches 6.5×10^{-5} M, the diameter of the semicircle changes in the reverse direction. This is in accord with the result from voltammograms, i.e. when the CTAB concentration is higher than 6.5×10^{-5} M, the ion pairs of $K_3Fe(CN)_6$ and CTAB could separate out from the solution. The good superposition of the Nyqusit plots with the plots simulated from the equivalent circuit of Fig. 6 demonstrates that the proposed equivalent circuit could be reliably used to explore the adsorption of CTAB on disturbed SAMs.

Figure 8 shows the effect of CTAB concentration on the values of the equivalent elements in Fig. 6. The effect of CTAB concentration on R_l could be divided into two parts (Fig. 8a): when the CTAB concentration is lower than 1×10^{-6} M, R_l remains stable with the variation in CTAB concentration, reflecting the negligible interaction between CTAB and $K_3Fe(CN)_6$; at higher concentrations, R_l seems to have a linear relationship with CTAB concentrations up to 1×10^{-4} M, indicating that the conductivity of the electrolyte might be increased by the addition of CTAB. The linear relationship between R_l and CTAB concentration can be used to determine the CTAB interaction. The variation of R_{ct} with CTAB concentration is different and is similar to the voltammetric responses (Fig. 8b), i.e. R_{ct} decreases significantly in the range of 1×10^{-6} M to 1×10^{-5} M, and tends to be stable in the two extremes. This result proves that the structure of the electrode interface has a dominant influence on the charge transfer between the solution and the electrode. The decrease of R_{ct} with the increase of CTAB concentration may also suggest a catalytic action of CTAB on the redox reaction of $K_3Fe(CN)_6$. The good consistency between the data measured from the intercepts of the semicircles on the Nyqusit plots and the data obtained from the equivalent circuit confirm the validity of using this equivalent circuit to describe the structure of the disturbed n-alkanethiolate SAMs in the presence of CTAB.

According to Montgomery and Wirth [21], the adsorption of surfactants on alkanethiolate SAMs could make the hydrophobic SAMs more compact through interchain penetration between the long chains of the surfactants and the alkanethiolate, which may change the interface structure and the electric double layer. Thus, the variation of CTAB concentration in solution might change the value of Q_{dl}, which was used to describe the electric double layer. From Fig. 8c it is clear that the obvious transformation of the electric double layer occurs at CTAB concentrations higher than 1×10^{-5} M. Considering the monolayer adsorptive behavior at this concentration range, the conclusion could be drawn that not the monomer adsorption but the monolayer adsorption of surfactants on SAMs can effectively change the electric double layer of the SAM-modified electrode. Owing to the adsorption of positively charged CTAB, the charges on the electrode surface increase and the capacitor of the electric double layer or the value of $Y_{dl,0}$ is enlarged. At the same time, the adsorption of CTAB on compact SAMs makes the double electric layer looser as a whole. This explains the drop in the value of ϕ_{dl} and the enhanced deviation of the electric double layer from a pure capacitor. In the CTAB concentration range of 1×10^{-7} M to 1×10^{-4} M, the value of ϕ_{dl} is confined to the range of 0.81–0.85, which is close to 1, i.e. Q_{dl} is approximately a capacitor. This is consistent with the function of Q_{dl} as a capacitor in the equivalent circuit.

In the equivalent circuit, Q_w stands for the impedance involved in the diffusion process. When the CTAB concentration is lower than 1×10^{-6} M, ϕ_w and $Y_{w,0}$ change little and ϕ_w has values around 0.3 (see Fig. 8d). When the CTAB concentration increases from 1×10^{-6} M to 1×10^{-5} M, both ϕ_w and $Y_{w,0}$ increase rapidly with CTAB concentration. With a further concentration increase, ϕ_w and $Y_{w,0}$ tend to be stable. From Eqs. 2 and 4, the relationship between $Y_{w,0}$ and R_{ct} is deduced as:

$$Y_{w,0} = R_{ct}^{2\phi_w - 1} 2^{-\phi_w} \sigma^{-2\phi_w} \tag{5}$$

The above equation well explains the opposite variations of $Y_{w,0}$ and R_{ct} with the increase of CTAB concentration. These results are in accord with the voltammetric responses. Moreover, when the CTAB concentration is higher than 1×10^{-5} M, the value of ϕ_w varies near 0.45, i.e. Q_w resembles a Warburg impedance, or the effect of the diffusion process on the redox of $K_3Fe(CN)_6$ becomes dominant.

On the basis of the above discussions, it is clear that CTAB undergoes two different types of adsorptive behavior in the range of 1×10^{-7} M to 1×10^{-4} M: monomer adsorption at concentrations lower than 1×10^{-6} M and monolayer adsorption at concentrations higher than 1×10^{-5} M. Between these two extremes, the adsorption of CTAB on SAMs behaves midway. The good superposition of the values of R_{ct} obtained from the diameter of the semicircle on Nyquist plots
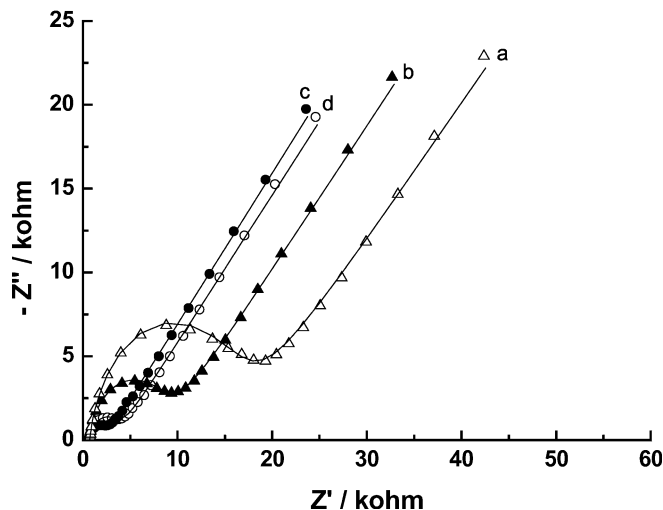

Fig. 9 Nyquist plots of 1 mM $K_3Fe(CN)_6$ at a disturbed n-dodecanethiolate SAM-modified gold electrode in the presence of: (*a*) 1×10^{-5} M LTAB; (*b*) 1×10^{-5} M CPB; (*c*) 1×10^{-5} M CTAB; (*d*) 1×10^{-5} M STAB. The *solid lines* were the fitting lines from the equivalent circuit in Fig. 6

and deduced from the equivalent circuit in Fig. 6 attests that this equivalent circuit is suitable to describe the adsorption of CTAB on disturbed hydrophobic SAMs. This conclusion is also supported by the approach of the value of ϕ_{dl} to 1 and the value of ϕ_w to 0.5.

The adsorption of a series of cationic surfactants with similar structures to CTAB on a disturbed n-alkanethiolate SAM-modified gold electrode

CTAB is a cationic surfactant composed of a long hydrophobic chain of methylene groups and a hydrophilic head of an ammonium salt. The adsorption of CTAB on hydrophobic SAMs is achieved through the interchain penetration of the long chains of CTAB and the SAMs. The length of the hydrophobic tails of the surfactants plays a critical role in their surface activity and adsorption strength on the interfaces. Figure 9 shows the Nyquist plots of a series of cationic surfactants at disturbed hydrophobic SAMs. The EIS plots change regularly with the length of the surfactant tails, except for STAB. Owing to its longer hydrophobic tail, STAB exhibits different adsorptive behavior from LTAB, CPB and CTAB, which is demonstrated by the fitting data from Fig. 9 to the equivalent circuit (Fig. 10). Except for STAB, the parameters of R_l, R_{ct} and ϕ_w in the equivalent circuit in the presence of cationic surfactants change linearly with the increase of the number of carbon atoms in the hydrophobic tails (n_c). The regularity of the other parameters is also apparent. This result supports the idea that the surface activity of surfactants is directly in relation to the length of their hydrophobic tails. The good consistency of the Nyquist plots of the four surfactants with the proposed equivalent circuit suggests that this equivalent circuit could
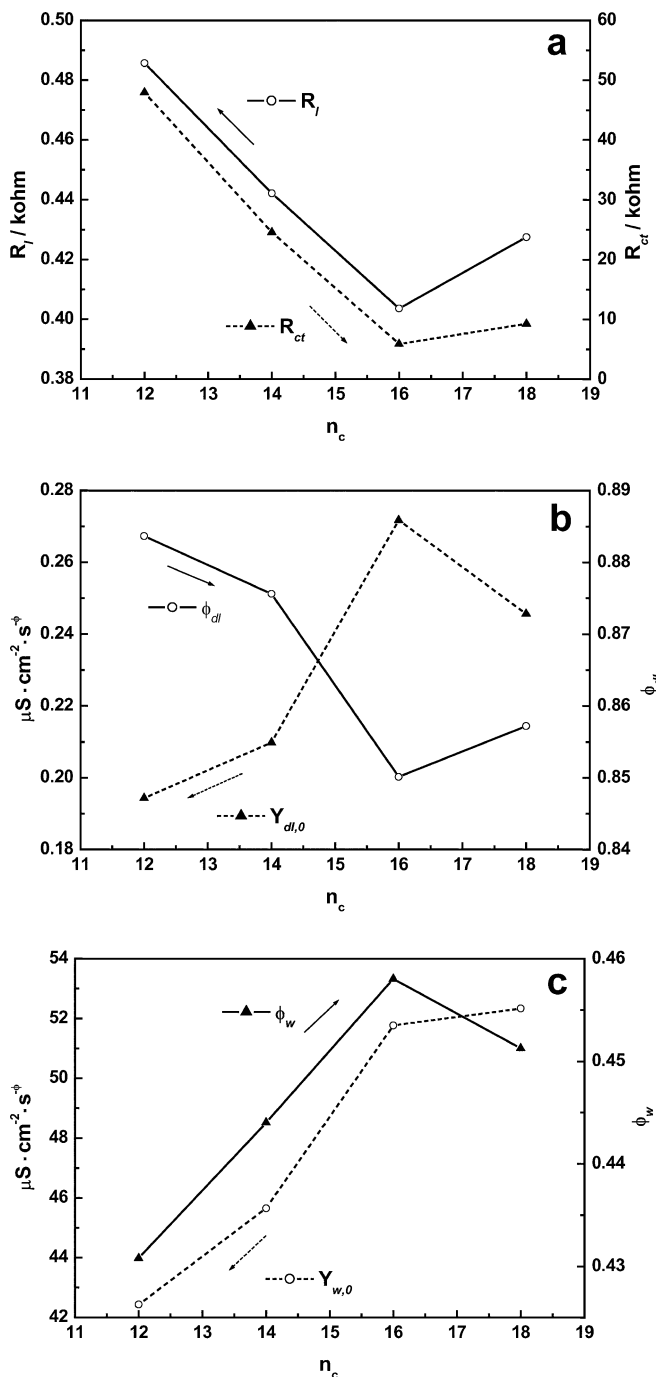
Fig. 10 The variation of the equivalent elements with the number of carbon atoms in the hydrophobic tails of a series of cationic surfactants obtained from Fig. 9: (**a**) R_l and R_{ct}; (**b**) Q_{dl}; (**c**) Q_w. The number of carbon atoms in CPB was regarded as 14 for convenient comparison

also be used to describe the adsorption of LTAB, CPB and STAB on disturbed n-alkanethiolate SAMs.

Conclusions

Investigation of the adsorption of cationic surfactants on hydrophobic disturbed n-alkanethiolate SAMs was

carried out by electrochemical methods. Compared with the completely restrained response at ordinary compact alkanethiolate SAMs, $K_3Fe(CN)_6$ showed a quasi-reversible response at disturbed SAMs. In the presence of cationic surfactants, the response of $K_3Fe(CN)_6$ was apparently improved. This phenomenon was employed to characterize the adsorption of cationic surfactants on hydrophobic SAMs. The effect of CTAB concentration on the voltammetric responses indicated that CTAB underwent two different types of adsorptive behavior on disturbed n-alkanethiolate SAMs: when the CTAB concentration was lower than 1×10^{-6} M, CTAB exhibited monomer adsorptive behavior; when the CTAB concentration was higher than 1×10^{-5} M, the adsorption of CTAB was as a monolayer; between the extremes, CTAB behaved midway. The EIS study showed that the adsorption of CTAB could be well fitted by a simple modified Randle's circuit, which consisted of two resistances and two CPEs. The effect of CTAB concentration on these equivalent elements demonstrated the adsorptive behavior of CTAB as proposed above. Moreover, the dependence of Q_{dl} on CTAB concentration revealed that not the monomer adsorption but the monolayer adsorption of CTAB could effectively influence the electric double layer of the electrode interface. Finally, the effect of the length of a series of cationic surfactants on their adsorption on disturbed n-alkanethiolate SAMs was investigated by EIS. The results suggested that the adsorptive behavior of these cationic surfactants was similar to CTAB. The surface activity of these surfactants increased with the increase of the length of their hydrophobic tails, except for STAB.

References

1. Rusling JF (1991) Acc Chem Res 24:75
2. Hu S, Yan Y, Zhao Z (1991) Anal Chim Acta 248:103
3. Yi H, Wu K, Hu S (2001) Talanta 55:1205
4. Zhang S, Wu K, Hu S (2002) Talanta 58:747
5. Hu S, Wu K, Yi H, Cui D (2002) Anal Chim Acta 464:209
6. Digua K, Kauffmann JM, Delplancke JL (1994) Electroanalysis 6:451
7. Digua K, Kauffmann JM, Delplancke JL (1994) Electroanalysis 6:459
8. Posac JR, Vazquez MD, Tascon ML, Acuna JA, Fuente CD, Velasco E, Batanero PS (1995) Talanta 42:293
9. Falaras P, Petridis D (1992) J Electroanal Chem 337:229
10. Nassar AF, Rusling JF, Kumosinski TF (1997) Biophys Chem 67:107
11. Carrero H, León LE (2001) Electrochem Commun 3:417
12. Hu C, Hu S (2004) Electrochim Acta 49:405
13. Wu K, Fei J, Hu S (2003) Anal Biochem 318:100
14. Sun Y, Fei J, Wu K, Hu S (2003) Anal Bioanal Chem 375:544

15. Wu K, Fei J, Bai W, Hu S (2003) Anal Bioanal Chem 376:205
16. Bianco P, Haladjian J (1997) Electrochim Acta 42:587
17. Mimica D, Zagal JH, Bedioui F (2001) Electrochem Commun 3:435
18. Wang L, Hu N (2001) J Colloid Interface Sci 236:166
19. Chattopadhyay K, Mazumdar S (2000) Bioelectrochemistry 53:17
20. Hu K, Bard AJ (1997) Langmuir 13:5418
21. Montgomery ME, Wirth MJ (1994) Langmuir 10:861
22. Sigal GB, Mrksich M, Whitesides GM (1997) Langmuir 13:2749
23. Montgomery ME, Green MA, Wirth MJ (1992) Anal Chem 64:1170
24. Montgomery ME, Wirth MJ (1992) Anal Chem 64:2566
25. Gerlache M, Senturk Z, Quarin G, Kauffmann JM (1997) J Solid State Electrochem 1:155
26. Kawaguchi T, Yamauchi Y, Maeda H, Ohmori H (1992) Anal Sci 8:691
27. Kawaguchi T, Yamauchi Y, Maeda H, Ohmori H (1993) Chem Pharm Bull 41:1601
28. Brug GJ, Van Den Eeden ALG, Sluyters-Rehbach M, Sluyters JH (1984) J Electroanal Chem 176:275
29. Retter U, Widmann A, Siegler A, Kahlert H (2003) J Electroanal Chem 546:87